

**Title:****Variable Offsetting of Polygonal Structures Using Skeletons****Authors:**

Martin Held, held@cosy.sbg.ac.at, Computerwissenschaften, University of Salzburg, Austria

Stefan Huber, stefan.huber@ist.ac.at, Institute of Science and Technology, Austria

Peter Palfrader, palfrader@cosy.sbg.ac.at, Computerwissenschaften, University of Salzburg, Austria

**Keywords:**

Voronoi diagram, Variable-radius offset

**DOI:** 10.14733/cadconfP.2015.231-235**Introduction:**

Offsetting is an important task in diverse applications in the manufacturing business. For a set  $C$  in the plane, the constant-radius offset with offset distance  $r$  is the set of all points of the plane whose minimum distance from  $C$  is exactly  $r$ . (We are interested in the Euclidean distance.) Formally, this offset curve can be defined as the boundary of the set  $\bigcup_{p \in C} B(p, r)$ , where  $B(p, r)$  denotes a disk with radius  $r$  centered at the point  $p$ . That is, the offset is the envelope of a set of disks of equal radius that have their centers along the input. Mathematically, the same offset curve can also be obtained as the Minkowski sum of  $C$  with a disk with radius  $r$  centered at the origin.

For polygons such an offset curve will consist of one or more closed curves made up of line segments and circular arcs, see Fig. 1, left. Held [3] describes how to use a Voronoi diagram, which is a versatile tool in computational geometry, to compute such an offset efficiently and reliably.

Mitered offsets differ from constant-radius offsets in the handling of non-convex vertices of an input polygon: Instead of adding circular arcs to the offset curve, the offset segments of the two edges incident to a non-convex vertex get extended until they intersect. This type of offset can be generated in linear time from a straight skeleton [4]. In order to avoid very sharp corners in the offset, the linear axis can be used in place of the straight skeleton [4], thus obtaining offsets with multi-segment bevels. See Fig 1, center and right.

A common feature of all these offsets is that the orthogonal distance of each offset element from its defining contour element is constant.

Several applications in industry, such as for garment manufacture, need to construct differently sized pieces from a single master design. One obvious method is to scale the master template accordingly. However, a naive approach would scale all elements equally, which need not always be good enough. (For instance, one might want to shrink the overall size of a shirt without necessarily shrinking its collar size by the same ratio.) A different approach to resizing is to use offsetting. To be able to control the offsetting process, a common demand is to create non-constant offsets, i.e., offset curves where the distance to the original input curve varies along that input. Brush stroke generation is another sample application that benefits of variable-distance offsets.

Variable-distance offset curves and surfaces are known in the literature. See, for instance, the work by Qun and Rokne [5] or Rossignac and Zhuo [6, 7]. However, prior art seems to concentrate on defining and comparing different offsets and is less concerned with efficiently or robustly computing offset curves. One common approach to constructing variable offsets seems to be based on sampling. Rendering-based methods also are feasible for sketching such offsets by means of a graphics hardware. However, they incur the additional problem of having to extract the actual offset curves from the rendered images.

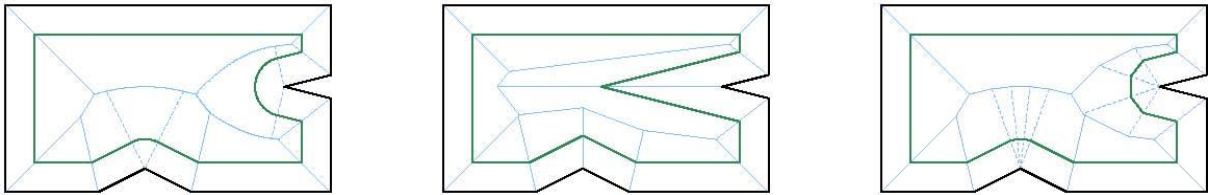


Fig. 1: (Left) The Voronoi-diagram (blue) of an input polygon  $p$  (black) enables efficient computation of the constant-radius offset. One interior offset curve of  $p$  is shown in green. The offset curve consists of line segments and circular arcs, and any point on it is at the same distance from the input in the standard Euclidean distance. (Center) The offset induced by the straight skeleton (blue) can have sharp corners that are far away from their respective input vertex in the standard Euclidean distance. (Right) Offsetting using the linear axis (blue) bevels the offset compared to the one induced by the straight skeleton. The offset still consists only of line segments.

#### Main Idea:

Consider a set  $S$  of vertices in the Euclidean plane and line segments between some pairs of these vertices. The line segments may share common endpoints but they may not intersect otherwise. (In computational geometry, such an input is called a planar straight-line graph, PSLG.) Let us denote by  $\bar{S} \subset \mathbb{R}^2$  the set of points covered by all vertices and line segments of  $S$ . Furthermore, we consider a weight function  $\sigma: \bar{S} \rightarrow \mathbb{R}^2$  that assigns to each vertex  $p$  of  $S$  a positive weight  $\sigma(p)$  and for each point on a line segment  $\overline{pq}$  of  $S$  we linearly interpolate its weight along  $\overline{pq}$  from  $\sigma(p)$  at  $p$  to  $\sigma(q)$  at  $q$ .

We now place a disk at each point  $p$  of  $\bar{S}$ . In analogy to the so-called prairie fire model, all disks have initially radius zero. As time increases, however, the radius of each disk grows proportional to the weight  $\sigma(p)$  of its center point  $p \in \bar{S}$ . The variable-radius offset for a given time is the envelope of this set of disks. As intended, input sites with small weight will induce an offset that is closer to them, and input sites that were assigned larger weights will cause their offsets to be farther away. Formally, this offset is the boundary of the set  $\bigcup_{p \in \bar{S}} B(p, \sigma(p) \cdot t)$ . Note that the term  $\sigma(p) \cdot t$  replaces the constant radius  $r$  from the previous section.

Our experience with using skeletal structures, such as the Voronoi diagram and the straight skeleton, to construct constant-radius and mitered offsets motivated us to look for another Voronoi-like structure to facilitate the computation of non-constant offsets. It turns out that the variable-radius Voronoi diagram introduced below is such a useful structure. It is defined relative to both weighted points and variably-weighted line segments.

*Preliminaries:* The Voronoi diagram  $\mathcal{VD}(S)$  of a set  $S$  of points in the plane, called sites, tessellates the plane into interior-disjoint regions. Each so-called Voronoi region belongs to exactly one site. The Voronoi region of a site  $s$  is given by the loci of all points in the plane whose closest site is  $s$ . The border between any two Voronoi regions lies on a straight line, namely the bisector of the regions' sites, see Fig. 2, left.

The prairie fire analogy illustrates this concept: Suppose that fires start in different locations on the prairie and that each fire expands into all directions, propagating at uniform speed. A point in the prairie then belongs to the region of the particular fire which reached it first.

Voronoi diagrams have been generalized in several different ways, such as using a different distance measure (e.g., Manhattan distance instead of Euclidean distance), choosing different types of input sites instead of just points (e.g., line segments or circular arcs), or assigning both additive and multiplicative weights to sites. In the prairie fire analogy, the latter generalization corresponds to starting certain fires sooner or have some spread faster. Figure 2, right, shows the Voronoi diagram of a multiplicatively weighted point set.

*Variable-radius Voronoi diagram:* We introduce the variable-radius Voronoi diagram  $\mathcal{VD}_v(S)$  as a generalized Voronoi diagram with generalizations into two directions: first, the set  $S$  of input sites is a

set of both vertices and (non-intersecting) line segments between pairs of these vertices, i.e., a planar straight-line graph. Second, we assign multiplicative weights to these sites. As described above, a vertex  $s \in S$  is assigned a positive weight  $\sigma(s)$ , and the weight of a point on a line segment  $\overline{pq}$  changes linearly between its endpoints from  $\sigma(p)$  to  $\sigma(q)$ . The distance of a point  $u$  in the plane to a vertex site  $s$  is defined as the Euclidean distance from  $u$  to  $s$ , divided by the weight of that site:  $d(u, s) := \|u - s\|/\sigma(s)$ . The distance of  $u$  to a line-segment site  $\overline{pq}$  is naturally defined as the minimum distance of  $u$  to any point of the line segment:  $d(u, \overline{pq}) := \min_{v \in \overline{pq}} \|u - v\|/\sigma(v)$ . While this may seem unwieldy at first, we can show that  $d(u, \overline{pq})$  can be computed easily using elementary geometry.

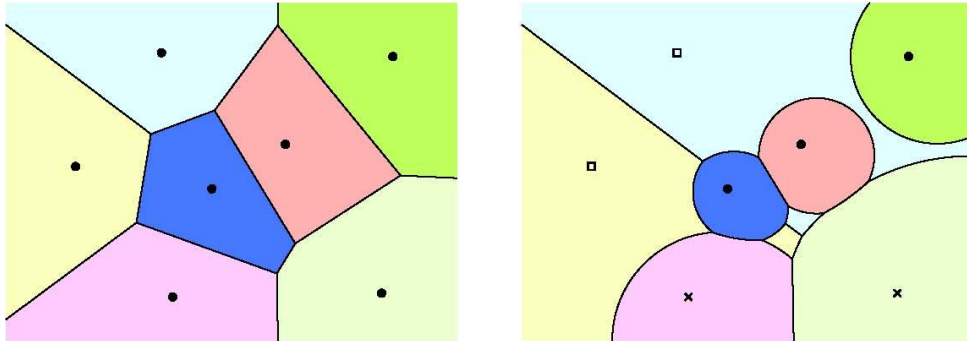


Fig. 2: (Left) The Voronoi diagram of a point set. Each site's Voronoi region is shaded in a different color. (Right) A multiplicatively weighted Voronoi diagram of the same point set. Vertices marked with a box have been assigned a weight of 3.0, those marked with a cross have weight 1.5, while the vertices shown with a disk have a weight of 1.0. The bisectors of vertices of different weights lie on circular arcs. Note that some Voronoi regions are disconnected.

As in the case of the standard Voronoi diagram, any point in the plane is in the (generalized) Voronoi region of the site that it is closest to. An arc that separates two regions comprises all points that have the same distance to two sites and a larger distance to all other sites.

The variable-radius Voronoi diagram inherits several important properties from the multiplicatively weighted Voronoi diagram of points. In particular, the region of a given site need not be connected, cf. Fig. 2 (right). That is, the region of a site may comprise two or more disconnected faces in the Voronoi diagram. Furthermore, bisectors between two vertices are circles or circular arcs [2]. Other bisectors, however, are more complex curves in general. A special case is given by the bisector between a vertex and a line segment of constant weight: It will be a conic section where the vertex site is a focus point and the supporting line of the segment site is the directrix of the conic. Depending on the ratio of the weights of the segment and the vertex, the bisector will either be an ellipse, a parabola, or a hyperbola.

The bisectors of a line segment  $\overline{pq}$  between the input vertices  $p$  and  $q$  exhibit another interesting property: They are full circles whose diameters on the line supporting  $\overline{pq}$  are bounded by a common point and their individual defining point-site, see Fig. 3, left.

*Offsetting:* While the bisectors of  $\mathcal{VD}_v(S)$  consist also of non-trivial curves, it can be shown that the variable-radius offset itself comprises line segments and circular arcs only. In particular, in Voronoi regions that belong to line-segment sites the offset will be a line segment also, whereas in regions associated with vertices the offset element will be a circular arc, see Fig. 3, right. We can compute this variable-radius offset of  $S$  for a given time  $t$  from the variable-radius Voronoi diagram  $\mathcal{VD}_v(S)$ . The approach is identical to how constant-distance offsets are computed based on Voronoi diagrams or straight skeletons [3, 4]. Roughly, we iterate through all the arcs of  $\mathcal{VD}_v(S)$  and add offset elements in each face that contains points at distance  $t \cdot \sigma$ . The topological information encoded in  $\mathcal{VD}_v(S)$  enables us to do this in time linear in the size of the Voronoi diagram and in a single iteration, without the

need to compute all pair-wise self-intersections of offsets. Furthermore, no detection and removal of invalid loops is required, no matter how large an offset distance is requested.

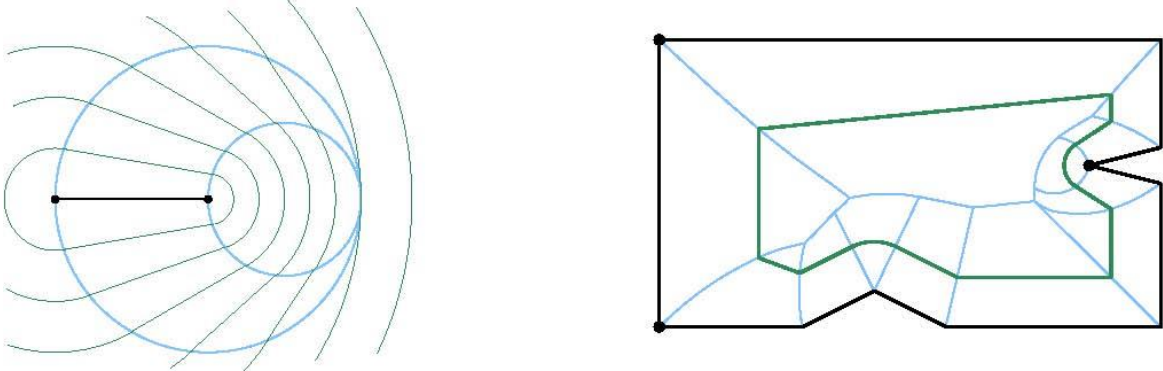


Fig. 3: (Left) The variable-radius Voronoi diagram (blue) of a simple input of two vertex sites and their connecting line segment (black). A family of offset curves is shown in green. (Right) The variable-radius Voronoi diagram inside a polygonal input. The marked input vertices on the left have been assigned a weight of 2.0 while the single marked vertex on the right has a weight of 0.5. All other vertices were given the standard weight of 1.0. A single offset curve is drawn in green.

*Implementation:* We developed a proof-of-concept C++ code that approximately computes the variable-radius Voronoi diagram of planar straight-line graphs. Our implementation is based on CGAL [1]. It also allows us to construct variable-radius offsets.

#### Conclusion:

We investigate one specific variant of a skeletal structure which we call the variable-radius Voronoi diagram. While this structure is of particular interest in itself, we demonstrate its applicability to robustly constructing variable-radius offsets.

A remaining open problem is to generalize the class of input sites to include circular arcs in addition to just line segments and vertices. The hope is that this would enable offsets that are  $G^1$  continuous for appropriate  $G^1$  inputs. However, note that the offset of a variable-weighted circular arc is not a circular arc. Hence, a better understanding of the mathematical characteristics of the resulting offsets and of the corresponding Voronoi bisectors is required.

#### Acknowledgements:

This work was supported by Austrian Science Fund (FWF): P25816-N15.

#### References:

- [1] CGAL, Computational Geometry Algorithms Library. <http://www.cgal.org/>.
- [2] Aurenhammer, F.; Edelsbrunner, H.: An Optimal Algorithm for Constructing the Weighted Voronoi Diagram in the Plane, *Pattern Recognition*, 17(2), 1984, 251-257. [http://dx.doi.org/10.1016/0031-3203\(84\)90064-5](http://dx.doi.org/10.1016/0031-3203(84)90064-5).
- [3] Held, M.: *On the Computational Geometry of Pocket Machining*, LNCS, Volume 500, Springer, 1991. <http://dx.doi.org/10.1007/3-540-54103-9>. ISBN 978-3-540-54103-5.
- [4] Palfrader, P.; Held, M.: Computing Mitered Offset Curves Based on Straight Skeletons, *Comp.-Aided Design & Appl.*, 2015. <http://dx.doi.org/10.1080/16864360.2014.997637>.
- [5] Qun, L.; Rokne, J. G.: Variable-Radius Offset Curves and Surfaces, *Mathl. Comput. Modelling*, 26(7), October 1997, 97-108. [http://dx.doi.org/10.1016/S0895-7177\(97\)00188-X](http://dx.doi.org/10.1016/S0895-7177(97)00188-X).
- [6] Rossignac, J.: *Ball-Based Shape Processing*, I. Debled-Rennesson; E. Domenjoud; B. Kerautret; P. Even (Editors), *Proc. 16th Int. Conf. Discrete Geom. Comp. Imagery (DCGI 2011)*, LNCS, volume

6607. Springer, Nancy, France, April 2011, 13-34. [http://dx.doi.org/10.1007/978-3-642-19867-0\\_2](http://dx.doi.org/10.1007/978-3-642-19867-0_2).
- [7] Zhuo, W.; Rossignac, J.: Curvature-based Offset Distance: Implementation and Applications, *Computers & Graphics*, 36(5), August 2012, 445-454. <http://dx.doi.org/10.1016/j.cag.2012.03.013>.